Japanese Journal of Applied Physics **51** (2012) 02BD06 **REGULAR PAPER**
DOI: 10.1143/JJAP.51.02BD06

Effect of Resistance Drift on the Activation Energy for Crystallization in Phase Change Memory

Chiyui Ahn*, Byoungil Lee, Rakesh G. D. Jeyasingh, Mehdi Asheghi[1], Fred Hurkx[2], Kenneth E. Goodson[1], and H.-S. Philip Wong

Department of Electrical Engineering, Stanford University, Stanford, CA 94305, U.S.A.
[1]*Department of Mechanical Engineering, Stanford University, Stanford, CA 94305, U.S.A.*
[2]*NXP-TSMC Research Center, Kapeldreef 75, 3001 Leuven, Belgium*

Received September 26, 2011; revised November 2, 2011; accepted November 8, 2011; published online February 20, 2012

The crystallization properties of phase-change memory (PCM) in the presence of thermal disturbances are investigated with a novel micro-thermal stage. It is found that the recrystallization time due to thermal disturbances significantly varies depending on how the PCM cell drifts. The longer crystallization time is obtained following additional resistance drift, which can be described by an increase of the effective activation energy for crystallization. The possibility of achieving better retention in a PCM cell by allowing the PCM cell to drift for a longer time is demonstrated in this work. The activation energy changes at a rate of more than 1 eV/decade with varying time intervals below a second. As the ambient temperature gets higher, the effect of resistance drift on the crystallization process is diminished with respect to the dominant crystallization process which has a higher crystal growth rate at elevated ambient temperatures.

1. Introduction

Phase change memory (PCM) has been considered to be one of the most promising candidates for future non-volatile memory technology.[1–3] Although it has been studied toward the PCM with high speed of a few tens of nanoseconds with good endurance of about 10^9 cycles,[4] low power consumption of a few microamperes of programming currents,[5] and extremely small dimensions of less than 20 nm,[6] a lack of understanding of the many physical phenomena imposes difficulties on building multi-bit arrays of reliable PCM devices at higher operating temperatures. These physical phenomena include threshold switching, crystallization, and resistance drift of the PCM cell. In particular, the crystallization property of the phase-change memory has not been extensively studied so far. The crystallization process has a strong dependence on materials and device geometry and is random in nature.[7] In this work, we focus on the recrystallization of the PCM cell where a part of the amorphous phase-change material changes to the crystalline state due to thermal disturbances from the neighboring cells that are being programmed. This partial crystallization of the cell can be a serious issue causing retention failure.[8,9]

An important issue for the development of the multi-level PCM cell is the drift of the cell resistance whereby the cell resistance of the PCM cell evolves with time, leading to data loss. Many efforts have been made to understand and control drift in PCM devices[10,11] and more recently, a new drift-tolerant coding technique has been introduced in ref. 12. Resistance drift has been attributed to stress relaxation of the phase change material.[10] As such, resistance drift may be correlated with the crystallization process. In this paper, the dependence of the crystallization process on the resistance drift is studied at shorter time scales (μs) using a doped SbTe phase change alloy[13] and an on-chip micro-thermal stage (MTS).[8] It is shown that the effective activation energy barrier for crystallization can be tuned to suppress the recrystallization of phase change material by controlling the amount of resistance drift between the thermal disturbances.

*E-mail address: cyahn@stanford.edu

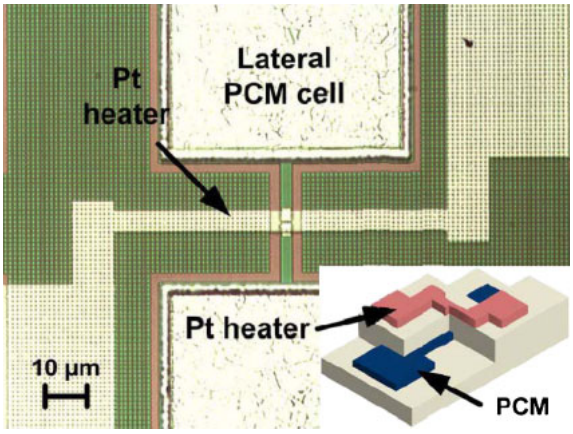

Fig. 1. (Color online) The top view microscope image of the lateral PCM cell bridged with the MTS platinum (Pt) heater. The inset shows the 3D bird's eye view. The SiO_x/SiN layer with thickness of about 1 μm is used for passivation between the PCM cell and the Pt heater.

2. Device Structures and Programming Setup

We use a device structure called Micro-Thermal Stage that has a platinum (Pt) heater built on top of the lateral PCM cell (see Fig. 1 for the device structure) to measure the crystallization time due to thermal disturbances in micro-second time scales. This MTS local heater allows us to study the crystallization behavior of the PCM cell at the short time scale comparable to that in the device operation. The detailed description of the device structure and the principles of operation were already published in ref. 8. The active PCM cell area bridged with a Pt heater is about $140 \times 400\,\text{nm}^2$, and the thickness of the phase change alloy is about 20 nm. The ambient temperature is controlled by changing the voltage amplitude of the heating pulse (V_{Pt} in Fig. 2). We calibrated the MTS temperature by obtaining the temperature dependence of the resistivity of the Pt heater (ρ_{Pt}), using

$$\rho_{\text{Pt}} = \rho_0 + TCR_{\text{Pt}}(T_{\text{HC}} + R_{\text{H}}P), \quad (1)$$

where TCR_{Pt}, T_{HC}, P, and R_{H} are temperature coefficient of resistance of Pt, the temperature of the hot chuck on which

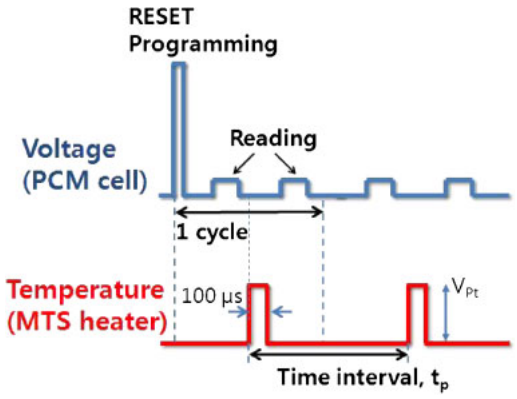

Fig. 2. (Color online) Electrical pulse profiles for RESET-programming, resistance reading, and MTS heating. Reading voltage (V_{READ}) is set at ~0.1 V to prevent the PCM cell from being recrystallized due to Joule heating. V_{Pt}, the voltage amplitude of the 100 μs-long heating pulse, is changed to give different annealing temperatures (T). The time interval t_p is fixed at 2 s otherwise mentioned. The effect of cell resistance drift on the crystallization time is taken into account by changing t_p.

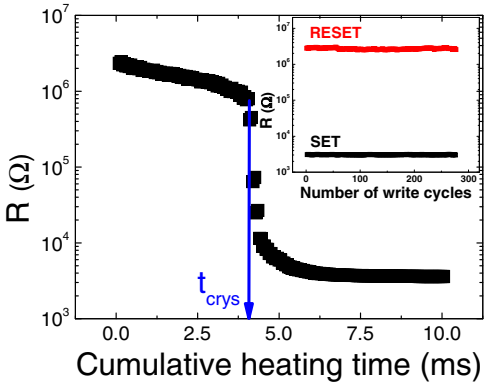

Fig. 3. (Color online) Crystallization due to thermal disturbances at $T \sim 270$ °C. Crystallization time (t_{crys}) is measured to be the cumulative heating time needed to form the first crystallization path within the amorphous region in the PCM cell. The inset shows the endurance characteristics with a high RESET/SET resistance ratio of ~1000.

the sample is placed, the power delivered to the Pt heater, and the thermal resistance between the Pt heater and the chuck, respectively. A constant R_H of about 1.06 °C/mW[8] is used in this work for the temperature ranges of interest (230–270 °C).

Figure 2 shows two sets of electrical pulses. One voltage pulse is directly applied to the PCM cell to RESET-program the cell initially and then read the resistances before and after the thermal disturbances afterwards. The other pulse is the 100-μs-long heating pulse that is applied to the platinum heater (MTS). The MTS pulse slowly recrystallizes the PCM cell and we count the number of heating pulses applied until the first crystallization path is formed inside the amorphous phase change material to determine the crystallization time. It should be noted that the multiple short heating pulses are considered in this study as additive thermal disturbances separated by a time interval t_p (see the electrical pulse setup at the bottom in Fig. 2) that can be controlled. The effect of resistance drift is incorporated here by changing t_p values as the resistance drift is related to time by a power-law relationship.[14] Though the temperature during the OFF periods of the MTS pulses is much smaller (room temperature) than that during the ON periods of the pulses, any difference in the number of applied MTS pulses and thus in crystallization time for different t_p values should come from the OFF periods of the MTS pulse because the ON periods of the MTS signal are maintained to be the exactly same for all different t_p cases.

3. Experimental Results and Discussion

Figure 3 shows the typical crystallization time (t_{crys}) measurement for a PCM cell as the cumulative heating time required to form the first crystallization path. With its own local MTS heater turned on (100 μs width, 1 μs rising/falling time, and 6 V voltage amplitude) for the temperature to be about 270 °C, the cell resistance gradually decreases until the crystallization path begins to form. By finding the point where the resistance begins to abruptly decrease during heating, the crystallization time is found to be about 4 ms in the figure. (We have found that any employed method to calculate the exact crystallization time makes little difference in our overall conclusion once it is consistently used.) Several hundred cycles of SET and RESET programming of the PCM cell are also shown in the inset to ensure that it has stable low- and high-resistance states (LRS and HRS, respectively).

To investigate the difference in t_{crys} for different time intervals (t_p), we changed the time interval from 1.2 to 4 s and the result is shown for the annealing temperature of about 260 °C in Fig. 4(a). It is clearly seen from the figure that the crystallization occurs slower by more than 20% when there is a second or more delay time between disturbances. The linear fit in the log-scaled t_{crys} versus t_p plot lies fairly well within the error bars of data, which enables us to conclude that the crystallization time due to thermal disturbances exponentially depends on the time interval between the multiple annealing pulses. It is well known that the resistance drift is governed by the phenomenological power law with time,[14] and thus we speculate from the result in Fig. 4(a) that the resistance drift can decelerate the recrystallization of the PCM cell.

Since the crystallization time also depends highly on the initial cell resistance which is related to the amorphous volume fraction, we had PCM cells programmed to different cell resistances (R) varying from 2 to 4 MΩ by applying a 100 ns-long voltage pulse with its amplitude increased in a few steps of mV, and measured the crystallization times for different t_p values of 1, 2, and 4 s in Fig. 4(b). Not surprisingly, it takes more time to be recrystallized into a low-resistance state for the PCM cell whose initial resistance is larger as seen in the figure. We also note that the effect of different amounts of resistance drift (different time intervals in the figure) becomes more significant when the PCM cell has larger R values due to the increased number of traps in amorphous region.[15]

In order to elucidate the physical origin of the observed dependence of crystallization time on the time interval between thermal disturbances, we studied in Fig. 5 how t_{crys} changes with different temperatures for longer time interval ranges of 1 to 1000 s. Figure 5 shows the typical Arrhenius plot of measured crystallization time versus the inverse of the thermal energy kT (where k is the Boltzmann constant)

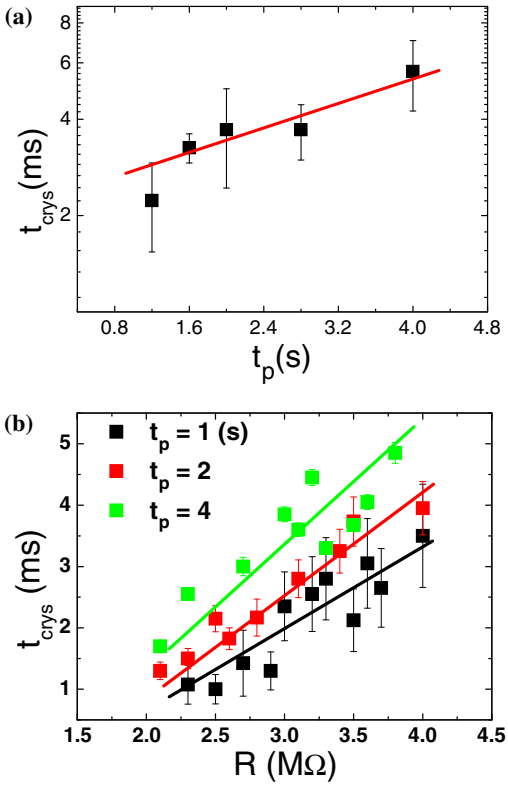

Fig. 4. (Color online) (a) Crystallization time as a function of the time interval t_p. (b) Initial cell resistance (R) dependence of crystallization time for three different time intervals. The annealing temperature is maintained at $T \sim 260\,^{\circ}\mathrm{C}$ in both (a) and (b). The red solid line in (a) and the dashed lines in (b) are drawn as linear fits. More than 10 samples of crystallization time measurements have been averaged for each data point to give statistically reasonable values with 1-sigma uncertainties.

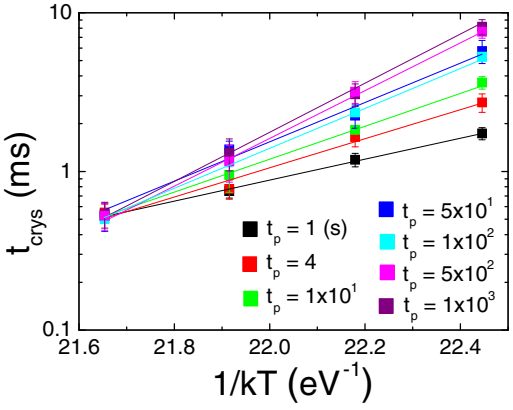

Fig. 5. (Color online) Crystallization time as a function of temperature (T). The slope of the t_{crys} versus $1/kT$ plot, which represents the activation energy, gets larger when we have a longer time interval t_p. The depicted lines are fits that show typical Arrhenius behavior, and the crystallization time was measured 5 times for each temperature to give statistical distribution.

for various temperatures. The activation energy (E_A) for crystallization, which is given by the slope of log-scaled t_{crys} versus $1/kT$ plot, is found to be related to the different amounts of resistance drift. The resistance drift in the experiment is controlled by varying the time interval t_p. This result implies that by allowing the PCM cell to drift for a longer time, the effective activation energy can be modulated to be higher in order to suppress the recrystallization.

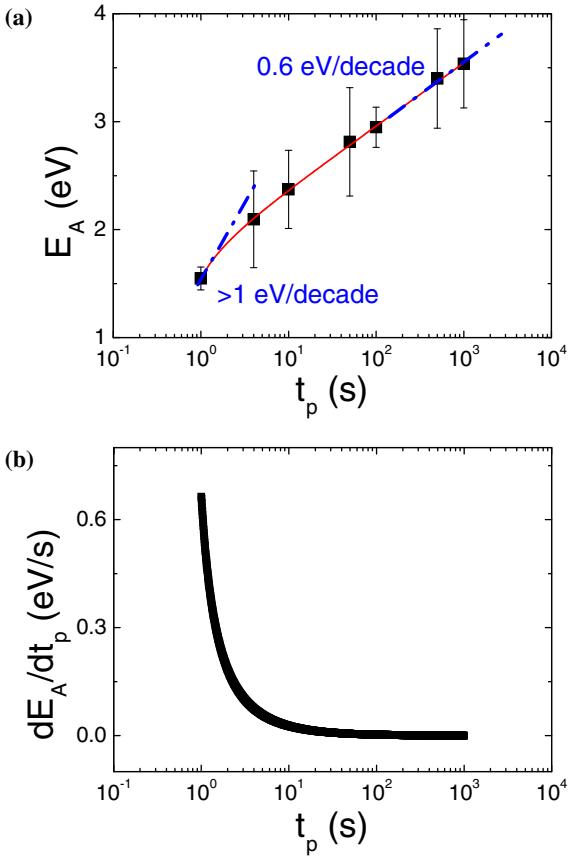

Fig. 6. (Color online) Change of the activation energy with different t_p values ranging from 1 s to 10^3 s, showing (a) E_A versus t_p and (b) dE_A/dt_p versus t_p. Due to quite large statistical variations, the E_A measurement was repeated about 20 times for each time interval. All depicted lines are guided for the eye. Activation energy E_A increases for longer t_p, but the increase rate (dE_A/dt_p) of the activation energy gets smaller for larger t_p values.

Figure 6 demonstrates more clearly how the effective energy E_A changes with the time interval t_p by plotting both the activation energy E_A and the increase rate of the activation energy dE_A/dt_p with varying t_p values in Figs. 6(a) and 6(b), respectively. We observe in Fig. 6(a) that the activation energy increases with time intervals at a rate of between $\sim$0.6 and $\sim$1 eV/decade for t_p ranges of interest. It is even expected to have much higher increase rate for t_p values less than 1 s. It should be also noted from Fig. 6(b) that the increase rate of the activation energy becomes smaller for larger time intervals. This is possibly due to the reduced drift caused by stress relaxation over time.[10] For t_p values of larger than 10 s, the increase rate does not change significantly with varying t_p values, being less than 0.3 eV/s. Even though the activation energy modulation due to different amounts of resistance drift looks not so large, the small difference in E_A can result in large difference in total crystallized material[16] and consequently in crystallization time.

4. Physical Model: Meyer–Neldel and Johnson–Mehl–Avrami–Kolmogorov

For each of measured activation energies E_A for different t_p values of 1, 4, 10, 50, 100, 500, and 1000 s, we extracted the pre-exponential factor τ_0 by measuring the crystallization

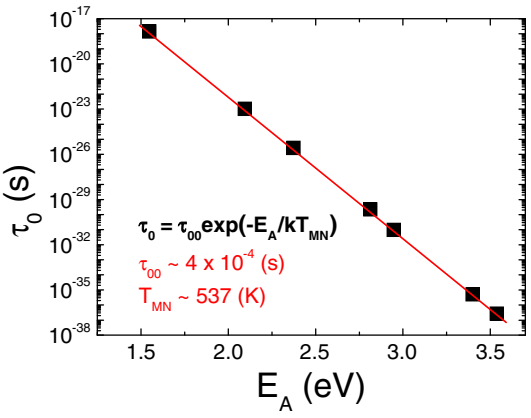

Fig. 7. (Color online) Meyer–Neldel plot of measured Arrhenius parameters of activation energy (E_A) and pre-exponential factor (τ_0) and fit with extracted parameters of τ_{00} and T_{MN}. τ_{00} and T_{MN} are found to be 4×10^{-4} s and 537 K.

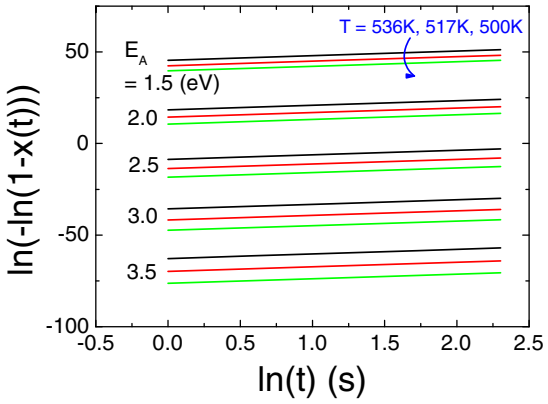

Fig. 8. (Color online) JMAK plot of $\ln\{-\ln[1-x(t)]\}$ versus lnt for different activation energy values of 1.5, 2.0, 2.5, 3.0, and 3.5 eV at $T = 536$ (black), 517 (red), and 500 K (green). $x(t)$ is the volume fraction of the crystallized material at time t.

time t_{crys} at a given temperature T and using the Arrhenius equation,

$$t_{crys} = \tau_0 \exp\left(\frac{E_A}{kT}\right). \quad (2)$$

Figure 7 shows that the measured Arrhenius parameters of τ_0 and E_A follow the Meyer–Neldel (MN) rule,[17] which is given as

$$\tau_0 = \tau_{00} \exp\left(-\frac{E_A}{kT_{MN}}\right). \quad (3)$$

The MN fit in Fig. 7 uses two fitting parameters of $T_{MN} \sim 537$ K and $\tau_{00} \sim 4 \times 10^{-4}$ s to describe the relationship of the pre-factor τ_0 in the Arrhenius equation with activation energy E_A. The energy Δ $(= kT_{MN})$ is of significant importance to understand the crystallization process within the framework of structural relaxation because it represents the thermal excitation energy provided by individual electron–phonon interaction for overcoming the activation barrier. τ_{00} is the crystallization time when the annealing temperature is the same as T_{MN}. As τ_0 decreases exponentially with E_A in eq. (3), the exponential increase of relaxation time on the activation energy found in eq. (2) is compensated by τ_0. This effect is called the MN effect or the compensation effect. The value of $\Delta \sim 46$ meV obtained from crystallization time measurements with additional resistance drift suggests that optical phonons-induced excitations with sufficient energy[18] should provide the energy Δ to overcome the activation energy barrier.

One of the prevailing descriptions of crystallization kinetics is the Johnson–Mehl–Avrami–Kolmogorov, or JMAK, theory.[19,20] It allows calculation of the volume fraction of crystallized material in terms of crystal nucleation and growth rates by

$$x(t) = 1 - \exp[-(kt)^n], \quad (4)$$

where t is time, n is the Avrami coefficient representing the dimensionality of the crystallization process, k is a constant describing nucleation and growth rate. k is generally related to the activation energy E_A by

$$k(T) = v \exp\left(-\frac{E_A}{k_B T}\right), \quad (5)$$

where v is the frequency factor. Since the activation energies range from ~1.5 to ~3 eV for different t_p values in the experiment, we draw the generic JMAK plots in Fig. 8 at three different temperatures of 536, 517, and 500 K for $v = 10^{22}$ s^{-1} and $n = 2.5$ for different activation energy values of 1.5, 2.0, 2.5, 3.0, and 3.5 eV. Again, we can see from the figure that small E_A difference results in huge difference in total crystallization fraction which supports the idea that small E_A modulation can change the recrystallization time significantly. Another important finding from Fig. 8 is that as T gets larger, the variations in total crystallization fraction with different E_A values becomes smaller. The thermal excitation model[21] can be confirmed by this result because electrons with higher thermal energy at elevated temperatures will more easily overcome the activation barrier and thus be less affected by the activation barrier height.

5. Conclusions

We presented an experimental demonstration of how resistance drift affects crystallization properties using a Micro-thermal Stage. The exponential dependence of the recrystallization time on the time interval allowed for resistance drift has been found. It would be better to raise the activation energy for crystallization by programming the neighboring cell at a later time in order to have better retention in a PCM cell. This would lower the possible retention failure due to thermal disturbances. MN and JMAK theories support the idea that crystallization kinetics can be explained by the thermal excitation model.[21]

Acknowledgements

This work is supported in part by NXP through the Stanford Center for Integrated Systems (CIS) custom research program, member companies of the Nonvolatile Memory Technology Research Initiative (NMTRI) at Stanford, the National Science Foundation (NSF) through grant CBET-0853350, and the MSD Focus Center, one of the six research centers funded under the Focus Center Research Program (FCRP), a Semiconductor Research Corporation entity.

1) S. Lai: IEDM Tech. Dig., 2003, p. 255.
2) Y. C. Chen, C. T. Rettner, S. Raoux, G. W. Burr, S. H. Chen, R. M. Shelby, M. Salinga, W. P. Risk, T. D. Happ, G. M. McClelland, M. Breitwisch, A. Schrott, J. B. Philipp, M. H. Lee, R. Cheek, T. Nirschl, M. Lamorey, C. F. Chen, E. Joseph, S. Zaidi, B. Yee, H. L. Lung, R. Bergmann, and C. Lam: IEDM Tech. Dig., 2006, p. 346910.
3) M. Breitwisch, T. Nirschl, C. F. Chen, Y. Zhu, M. H. Lee, M. Lamorey, G. W. Burr, E. Joseph, A. Schrott, J. B. Philipp, R. Cheek, T. D. Happ, S. H. Chen, S. Zaidr, P. Flaitz, J. Bruley, R. Dasaka, B. Rajendran, S. Rossnage, M. Yang, Y. C. Chen, R. Bergmann, H. L. Lung, and C. Lam: VLSI Tech. Symp., 2007, p. 100.
4) J. Lee, S. Cho, D. Ahn, M. Kang, S. Nam, H.-K. Kang, and C. Chung: IEEE Electron Device Lett. **32** (2011) 1113.
5) F. Xiong, A. D. Liao, D. Estrada, and E. Pop: Science **332** (2011) 568.
6) S. Raoux, G. W. Burr, M. J. Breitwisch, C. T. Rettner, Y.-C. Chen, R. M. Shelby, M. Salinga, D. Krebs, S.-H. Chen, H.-L. Lung, and C. H. Lam: IBM J. Res. Dev. **52** (2008) 465.
7) U. Russo, D. Ielmini, A. Redaelli, and A. L. Lacaita: IEEE Trans. Electron Devices **53** (2006) 3032.
8) S. Kim, B. Lee, M. Asheghi, F. Hurkx, J. P. Reifenberg, K. E. Goodson, and H.-S. P. Wong: IEEE Trans. Electron Devices **58** (2011) 584.
9) A. Redaelli, D. Ielmini, U. Russo, and A. L. Lacaita: IEEE Trans. Electron Devices **53** (2006) 3040.
10) M. Mitra, Y. Jung, D. S. Gianola, and R. Agarwal: Appl. Phys. Lett. **96** (2010) 222111.
11) M. Boniardi, D. Ielmini, S. Lavizzari, A. L. Lacaita, A. Redaelli, and A. Pirovano: IEEE Trans. Electron Devices **57** (2010) 2690.
12) N. Papandreou, H. Pozidis, T. Mittelholzer, G. F. Close, M. Breitwisch, C. Lam, and E. Eleftheriou: IEEE Int. Memory Workshop, 2011, p. 1.
13) M. H. R. Lankhorst, W. S. M. M. Ketelaars, and R. A. M. Wolters: Nat. Mater. **4** (2005) 347.
14) D. Ielmini, S. Lavizzari, D. Sharma, and A. Lacaita: IEDM Tech. Dig., 2007, p. 939.
15) G. B. Beneventi, A. Calderoni, P. Fantini, L. Larcher, and P. Pavan: J. Appl. Phys. **106** (2009) 054506.
16) S. Senkader and C. D. Wright: J. Appl. Phys. **95** (2004) 504.
17) W. Meyer and H. Neldel: Z. Tech. Phys. **12** (1937) 588.
18) A. Yelon, B. Movaghar, and H. M. Branz: Phys. Rev. B **46** (1992) 12244.
19) W. A. Johnson and R. F. Mehl: Trans. AIME **135** (1939) 416.
20) M. Avrami: J. Chem. Phys. **7** (1939) 1103.
21) D. Ielmini, M. Boniardi, A. L. Lacaita, A. Redaelli, and A. Pirovano: Microelectron. Eng. **86** (2009) 1942.